Stem Cell Reports
Article

OPEN ACCESS

Replicable Expansion and Differentiation of Neural Precursors from Adult Canine Skin

Thomas Duncan,[1] Aileen Lowe,[1,2] Kuldip Sidhu,[2] Perminder Sachdev,[3,4] Trevor Lewis,[5] Ruby C.Y. Lin,[5] Vladimir Sytnyk,[6] and Michael Valenzuela[1,*]

[1]Regenerative Neuroscience Group, Brain and Mind Centre, University of Sydney, Sydney, NSW 2050, Australia
[2]Stem Cell Laboratory, University of New South Wales, Sydney, NSW 2031, Australia
[3]Centre for Healthy Brain Ageing, University of New South Wales, Sydney, NSW 2031, Australia
[4]School of Psychiatry, University of New South Wales, Sydney, NSW 2052, Australia
[5]School of Medical Sciences, University of New South Wales, Sydney, NSW 2052, Australia
[6]School of Biotechnology and Biomolecular Science, University of New South Wales, Sydney, NSW 2052, Australia
*Correspondence: michael.valenzuela@sydney.edu.au
http://dx.doi.org/10.1016/j.stemcr.2017.07.008

SUMMARY

Repopulation of brain circuits by neural precursors is a potential therapeutic strategy for neurodegenerative disorders; however, choice of cell is critical. Previously, we introduced a two-step culture system that generates a high yield of neural precursors from small samples of adult canine skin. Here, we probe their gene and protein expression profiles in comparison with dermal fibroblasts and brain-derived neural stem cells and characterize their neuronal potential. To date, we have produced >50 skin-derived neural precursor (SKN) lines. SKNs can be cultured in a highly replicable fashion and uniformly express a panel of identifying markers. Upon differentiation, they self-upregulate neural specification genes, generating neurons with basic electrophysiological functionality. This unique population of neural precursors, derived from mature skin, overcomes many of the practical issues that have limited clinical translation of alternative cell types. Easily accessible, neuronally committed, and patient specific, SKNs may have potential for the treatment of brain disorders.

INTRODUCTION

Profound neuronal and synaptic loss is a hallmark of neurodegenerative disorders and is the best pathological correlate of cognitive impairment in Alzheimer's disease (AD) (Terry et al., 1991; Scheff and Price, 2006). Restoration of depleted neuronal populations with stem cell therapy is a promising treatment strategy (Daley, 2012; Lindvall et al., 2012; Duncan and Valenzuela, 2017), but the inaccessibility of endogenous neural stem cells within the brain's neurogenic niches means that alternative cell sources are required, preferably of autologous origin, to avoid long-term immunosuppression, which is harmful to both graft and host.

Reprogramming technology transformed the field, converting fibroblasts (FBTs) and other somatic cells into induced pluripotent stem cells (iPSCs) (Takahashi and Yamanaka, 2006) capable of generating functional neurons *in vivo* (Wernig et al., 2008). Alternatively, somatic cells can be converted directly into induced neurons (iNs), in effect bypassing the pluripotent state by induced upregulation of neuronal specification genes *ASCL1*, *NEUROD*, *MYTL*, and *BRN2* (Pang et al., 2011; Pfisterer et al., 2011). However, clinical translation of reprogramming technology remains limited for a number of reasons. First, conversion efficiency is typically very low, <1% of initial cells for iPSCs (Liao et al., 2008) and <6% for iNs (Pang et al., 2011). Second, both cell types suffer from unacceptably high line-to-line (and even clone-to-clone) variability (Truong et al., 2016), a factor that precludes clinical translation. Third, the unlimited capacity of iPSCs to self-renew presents an inherent risk of uncontrolled cell growth *in vivo*, with high (60%) tumor rates reported (Ring et al., 2012). Finally, genetic modification raises significant safety concerns, including activating oncogenes and the risk of unanticipated mutagenesis.

The discovery of niches within adult skin that continue to harbor multipotent stem cells raised the prospect of overcoming some of these limitations. Cell populations within these niches exhibit stem cell-like properties, distinct from mesenchymal or hematopoietic stem cells, and retain a neurogenic developmental potency without genetic manipulation, including expression of neural stem cell-related proteins such as NESTIN and SOX2 *in situ* (Toma et al., 2001; Fernandes et al., 2004). Using a neurosphere propagation method, these native stem cell-like cells, termed skin-derived precursors (SKPs), can be expanded for multiple passages (>50), and mature into neural cell types when exposed to neurodifferentiation factors (Toma et al., 2001; Biernaskie et al., 2006; Lavoie et al., 2009). However, the final neuronal yield achieved by this approach has been very low (2%–10% across studies), and the propensity for glial cell differentiation (Toma et al., 2005; Hunt et al., 2008) has generally excluded translation of SKP cells to neuronal therapeutic application.

Responding to this, we previously reported enhanced cellular homogeneity and neurogenic potential using a two-step neurosphere-adherent culture system that begins with mature adult canine skin (Valenzuela et al., 2008). The complex three-dimensional growth environment and

uneven exposure to growth signals inherent in the neurosphere assay permits and promotes heterogeneous cell growth (Bez et al., 2003; Babu et al., 2007), with neural stem cells reported to represent less than 1% of this population (Reynolds and Rietze, 2005). By contrast, we used neurospheres solely as a primary selection step, further expanding the resultant cells as an exclusively epidermal growth factor (EGF)/basic fibroblast growth factor (bFGF)-dependent adherent monolayer culture. Adherent expansion of human SKPs has been reported previously (Joannides et al., 2004), and while better neuronal yields were achieved using serum and astrocyte-conditioned medium, glial and mesenchymal cell types remained commonplace. Adherent culture systems have also been employed to expand brain-derived neural stem cells, producing more homogeneous cell populations biased toward GABAergic and glutamatergic neurons (Conti et al., 2005; Pollard et al., 2006; Goffredo et al., 2008). Combining these approaching in our two-step serum-free culture system, a unique population of skin-derived neural precursors (SKNs) can be routinely generated from adult canine skin, maturing to produce greater than 90% neuronal yields *in vitro* without genetic manipulation (Valenzuela et al., 2008). Accordingly, SKNs represent a promising candidate for autologous neural cell therapy.

Our choice of studying canine skin was intentional because of the poor history of translation of rodent research into effective human neurodegenerative treatment. Rodents do not naturally develop AD pathology or neurobehavioural signs in late life, and transgenic models have failed to predict outcomes in human clinical trials (Cummings et al., 2014; Breitner, 2015). By contrast, canine cognitive dysfunction (CCD) is a naturally occurring analogue of human AD; affected dogs display a progressive amnestic syndrome (Cummings et al., 1996; Salvin et al., 2011) as well as AD pathology (Cummings et al., 1996), and, as in humans, prevalence accelerates exponentially in old age (Salvin et al., 2010). CCD may therefore be an ideal translational model to test regenerative therapies. Yet prior to this, any candidate cell type needs thorough characterization. Here, we therefore assess the line-to-line replicability and neurogenic potential of canine SKNs in comparison with both canine dermal FBTs and brain-derived neural precursor cells (NPCs) isolated from the canine neurogenic niche.

RESULTS

SKNs Are Isolated and Expanded Using a Clinically Replicable Protocol

Our protocol for the culture of canine SKNs combines initial neurosphere selection with passage as an adherent monolayer for cellular homogenization (Figure 1A). From an approximately 6 cm^2 abdominal skin sample, under proliferative conditions, floating neurospheres ($\approx$100 μm in diameter) formed in culture within 7 days of isolation (Figure 1B). Following selection of these neurospheres, and their enzymatic dissociation, the resulting cells were cultured as an adherent monolayer. A large amount of cell death occurred within the first 2 days of this adherent culture, but a selective population consisting of exclusively EGF/bFGF-maintained SKNs survived. Following first passage, approximately 1,000,000 SKNs could be routinely generated from over 50 individual skin donors (85% donor-wise success rate). The clonal ability of SKNs was demonstrated by seeding at single-cell density in a collagen matrix that precluded cell fusion, with spheres approximately 50 μm in diameter forming after 7 days of culture (Figure 1C).

SKNs Demonstrate Limited Proliferative Capacity *In Vitro*

Under our adherent culture conditions, a homogeneous SKN population could be routinely expanded for up to five passages. At first and second passage, 80% confluence (passage density) was reached within 7 days, undergoing an average of 2.7 population doublings, defined as [log(final cell count/starting cell count)]/log(2) (Greenwood et al., 2004). Following third passage, proliferative rates began to decline, with only 1.4 population doublings occurring within an equivalent time frame. This decline was also quantified by 5-ethynyl-2′-deoxyuridine labeling of actively dividing cells. Initially comparable levels of active proliferation in SKNs and brain-derived NPCs significantly declined in the SKN cultures at passage 3 and beyond (Figure 1D). This observation was also consistent with *SOX2* gene expression, a regulator for stem cell proliferation, where expression in SKNs was significantly lower than in NPCs (*p = 0.01; Figure 1E). Under adherent proliferative conditions, SKNs are therefore limited in terms of their proliferative capacity.

SKNs Are a Distinct Population from Dermal FBTs

Global transcriptome analysis was carried out on canine dermal FBTs, SKNs, and NPCs, in order to better understand the neural potential of SKNs and the general relationship between these three cell types. Principle-component analysis of 32,000 transcripts accounted for 60.1% of total transcriptomic variance, with three cell populations observed, each with distinctive expression profiles (Figure 2A). Cell lines within cell types were highly correlated ($r \geq 0.98$ SKN, $r \geq 0.98$ NPC, $r \geq 0.98$ FBT), while globally SKN and FBT lines were more closely correlated (r range: 0.96–0.97) than SKN and NPC lines (r range: 0.92–0.94).

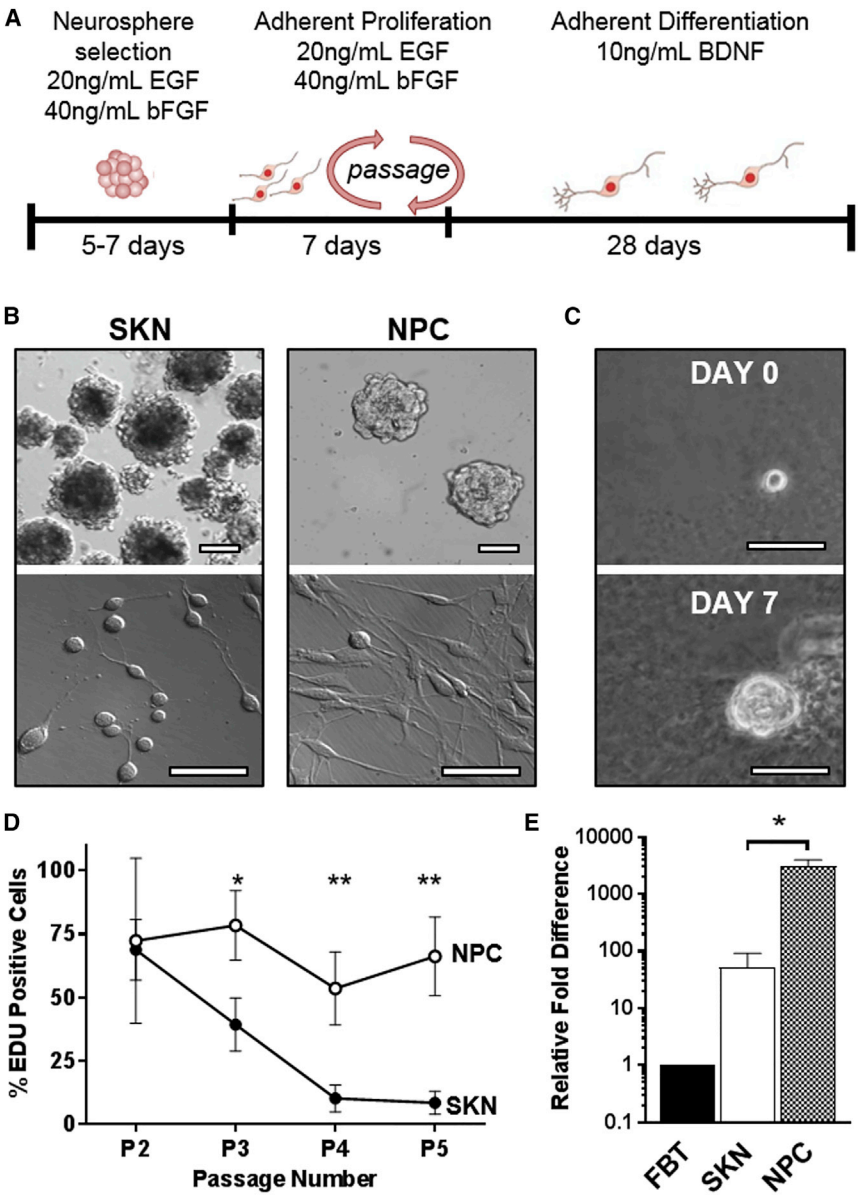

Figure 1. SKNs Are Rate Limited *In Vitro*

(A) SKN culture protocol and timing of differentiation.

(B) Representative morphology of adult canine SKNs and NPCs at the neurosphere stage (top) and during subsequent adherent monolayer expansion (bottom). Scale bars, 50 μm.

(C) Clonal proliferation from a single SKN cell. Scale bars, 50 μm.

(D) SKNs exhibit significantly lower expression of cell division marker 5-ethynyl-2′-deoxyuridine (EDU) at passage 3 and beyond compared with adult NPCs (P3, *p = 0.02; P4, **p = 0.008; P5, **p = 0.003; n = 3 independent experiments; mean ± SEM).

(E) Gene expression of master neural stem cell regulator *SOX2* in SKNs at passage 3 is intermediate between adult fibroblasts (FBT) and NPCs (*p = 0.01; n = 3 independent experiments; mean ± SEM).

Correlation coefficients for individual cell lines are displayed in Table S1.

To elucidate whether underlying molecular profiles were similar between these three cell types, ANOVA was performed at a false discovery rate of <0.05 to identify genes with a greater than 2-fold difference in normalized expression between cell types. Of the 32,000 genes analyzed, 291 genes were differentially expressed between SKNs and FBTs, while 2,157 genes were differentially expressed between SKNs and NPCs (Figure 2B). These univariate results indicate that SKNs are closer in global gene expression to FBTs than NPCs. A multivariate method of hierarchical clustering on differentially expressed genes also placed SKNs in a closer relationship to FBTs than NPCs (Figure 2C). Nevertheless, qPCR examination of specific neural stem and precursor markers showed that SKNs retain a distinct gene expression profile to FBTs, with *NES, P75NTR, DCX*, and *TUBB3* all significantly upregulated (Figure 2D). Moreover, from the Venn diagram we can infer that there are at least 40 genes specific to SKNs (detailed in Table S2). Many of these genes are associated with cell proliferation, adhesion, migration, and cytoskeletal organization. Of particular note were genes coding for protocadherins. These cell-adhesion proteins are predominantly expressed by the developing CNS (Sano et al., 1993), and have key roles in establishing neuronal connectivity and dendrite arborization (Schalm et al., 2010; Lefebvre et al., 2012).

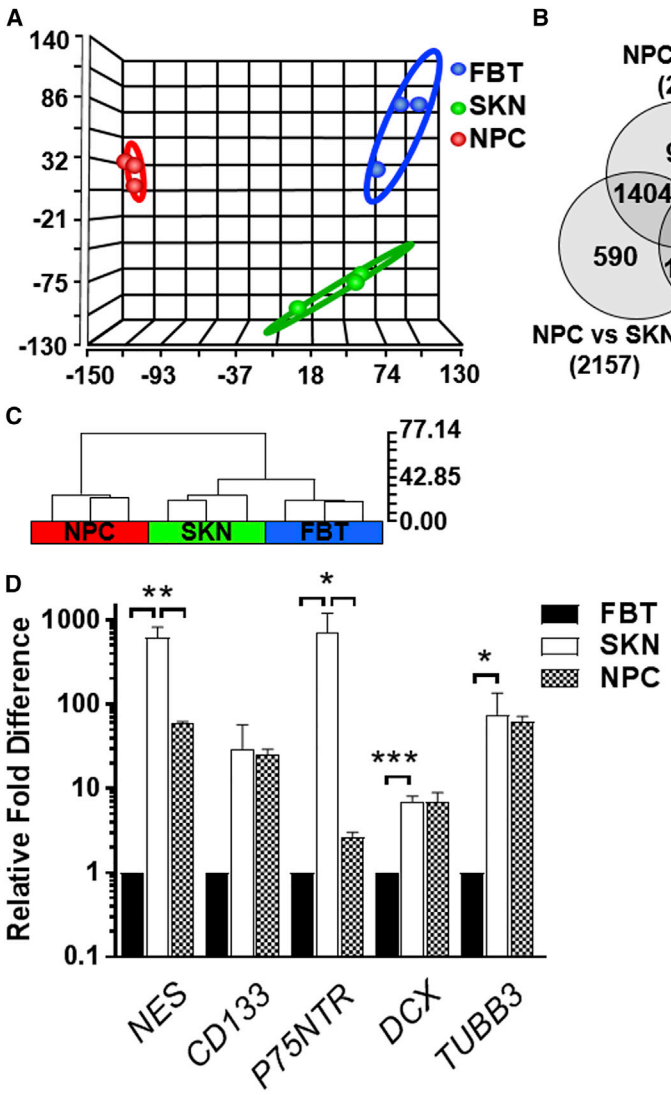

Figure 2. Gene Expression Patterns of SKNs Are Distinguished from FBTs or NPCs

(A) Principal components analysis of global gene expression of SKN, FBT, and NPC lines showed three distinct expression patterns. Further analysis indicated that gene expression from SKNs correlate closer to gene expression from FBTs than NPCs. See also Table S1 (n = 3 independent experiments; mean ± SEM).

(B) Univariate analysis shows SKNs and FBTs to have 291 differentially expressed genes and the least dissimilarities between cell types. Forty genes were expressed exclusively by SKNs. See also Table S2.

(C) Hierarchical clustering of significant differentially expressed genes based on Euclidean distance implicated that SKNs are globally closer to FBTs than NPCs.

(D) qPCR showed that SKNs have significantly higher transcript expression of neural stem cell-like marker gene *NES* (**p = 0.003), neural crest gene *P75NTR* (**p = 0.03), neuroblast gene *DCX* (***p = 0.0005), and immature neuronal gene *TUBB3* (*p = 0.04) compared with FBTs (n = 3 independent experiments; mean ± SEM).

Transcript lists containing the most commonly cited genes for pluripotency, neurogenesis, SKPs, mesenchymal stem cells (MSCs), growth factors, and growth factor receptors were compared for expression intensity between SKNs and NPCs (Figure 3). A full list of the individual gene expression fold changes between SKNs and NPCs can be found in Table S3. The iPSC pluripotency reprogramming factor *KLF4* (Takahashi and Yamanaka, 2006; Takahashi et al., 2007), and the *TBX3* gene implicated in embryonic stem cell proliferation and neuroepithelial differentiation (Esmailpour and Huang, 2012), were found to be upregulated in SKNs. Pluripotency markers *BUB1*, *TCL1A*, and *PRC1* were all upregulated in NPCs, confirming their greater proliferative capacity, as reported in Figure 1D. As expected, NPCs also showed stronger expression of neurogenesis markers. However, early neurogenesis markers *MKI67*, *PAX6*, *NCAM1*, *NES*, and *SOX2* were also strongly expressed in SKNs, indicative of a largely undifferentiated population of neural precursors. SKNs expressed the majority of SKP and MSC markers more intensely than NPCs, with significant upregulation of *PDGFRA*, *HOXA5*, *HOXC4*, *HOXC6*, *TWIST2*, *EYA1*, *MAB21L1*, *MSX1*, *RHOBTB3*, and *AP2A1*.

Growth factor and receptor gene expression were explored in order to gain insight into factors that SKNs may produce, or be responsive to, if transplanted in the brain. Interestingly, genes for insulin-like growth factors and their receptors were highly expressed in SKNs compared with NPCs. Furthermore, expression of *IL7* and *VEGFC* were upregulated in SKNs relative to NPCs. These growth factors, while expressed in adult skin, also have key roles in both the adult and developing brain, including neurogenesis and synaptogenesis, and as migratory cues for neuronal precursors (Michaelson et al., 1996; D'Ercole

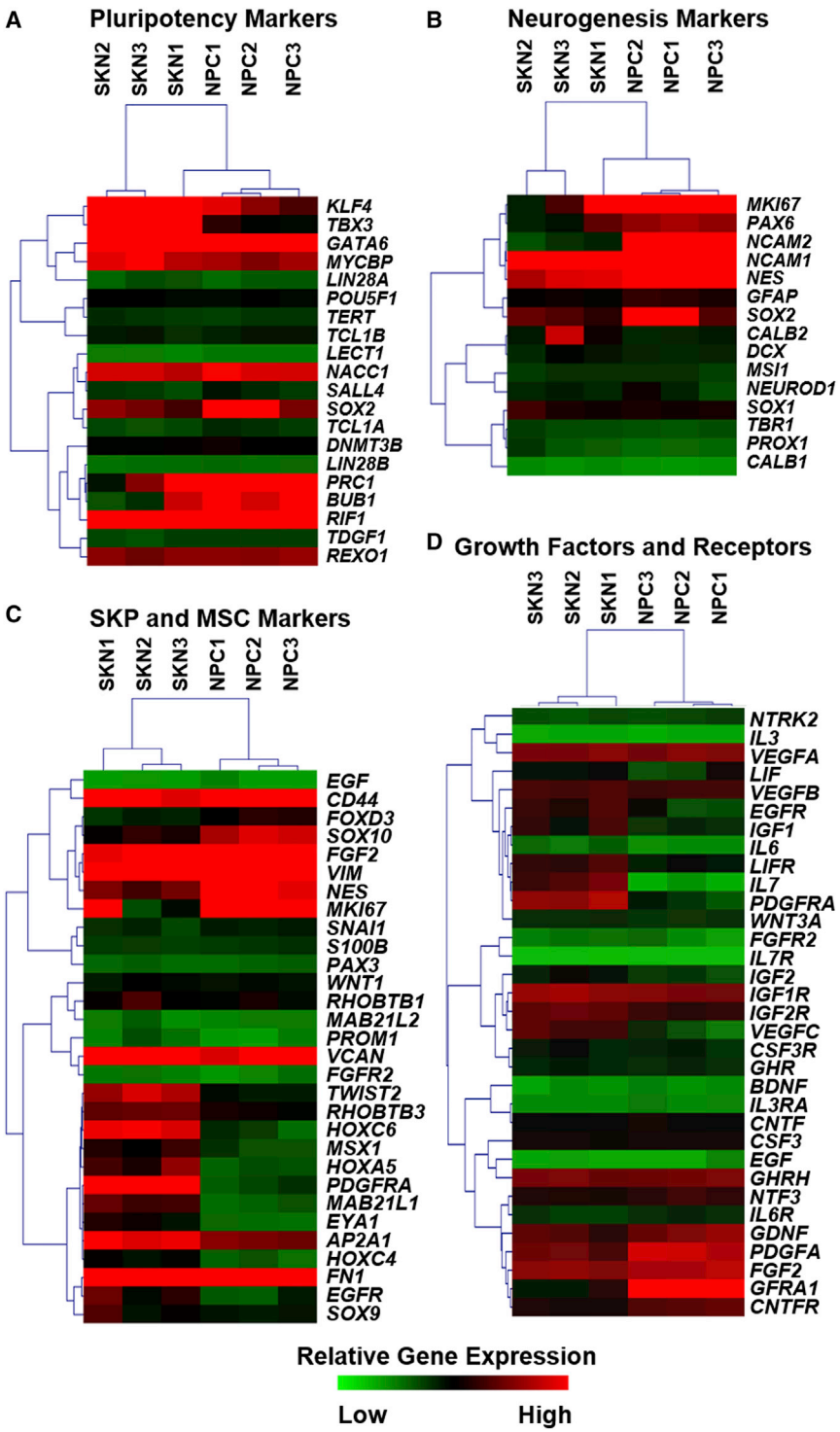

Figure 3. Gene Expression Heatmaps for NPC and SKN Lines

Heatmap of (A) pluripotency, (B) neurogenesis, (C) SKP and MSC, and (D) growth factor- and receptor-associated genes comparing NPC with SKN cell lines. Gene expression fold changes are color coded to visualize highly expressed genes. High relative expression of multiple genes associated with pluripotency and neurogenesis was evident in both SKN and NPC lines, while many SKP and MSC genes were expressed to a greater degree in SKNs, indicative of their dermal origins.

et al., 2002; Rosenstein et al., 2010). As such, they may facilitate SKN survival and engraftment following transplantation.

Pathway enrichment was then carried out on the 2,157 differentially expressed gene list (SKNs versus NPCs) and scored based on Fisher's exact test ($p < 0.01$) to identify functional groups with more than two over-represented genes from a specific pathway. Genes were referenced against the Kyoto Encyclopedia of Genes and Genomes *C. familiaris* genome database (Kanehisa et al., 2004). The

Table 1. Pathway Enrichment Analysis of Differentially Expressed Genes in SKN Cell Lines Based on the Kyoto Encyclopedia of Genes and Genomes Pathways

Pathway Name	Enrichment Score	Enrichment p Value	Percentage of Pathway Genes Represented
Focal adhesion	17.29	0.00000003	24
Extracellular matrix-receptor interaction	16.47	0.00000007	33
PI3K-Akt signaling pathway	11.90	0.000006	19
Proteoglycans in cancer	9.82	0.00005	30
Dilated cardiomyopathy	9.81	0.00005	20
Cell-adhesion molecules	9.57	0.00006	26
Actin cytoskeleton regulation	8.95	0.0001	23
Hypertrophic cardiomyopathy	8.89	0.0001	19
Keratan sulfate glycosaminoglycan biosynthesis	7.69	0.0004	26
Axon guidance	7.33	0.0006	47
Mitogen-activated protein kinase signaling pathway	7.16	0.0007	21
Pathways in cancer	4.95	0.007	17
Glycosphingolipid biosynthesis	4.81	0.008	15
Prostate cancer	4.66	0.009	30
Melanoma	4.61	0.01	20

PI3K, phosphatidylinositol 3-kinase.

aim was to characterize and compare the biological pathways best represented in both cell types. Focal adhesion, extracellular matrix (ECM)-receptor interaction and PI3-AKT signaling pathway were the three most enriched pathways (Table 1). The relative gene expression in SKNs and NPCs for components of these pathways and others have been mapped in Figures S1–S6. The focal adhesion pathway (Figure S1), incorporating upregulated expression of p21-activated kinase proteins in SKNs, has an important role in the regulation of the actin cytoskeleton and is implicated in cell proliferation and migration, mediating filopodia formation, and cell motility (Xia et al., 2008). Interlinked with the focal adhesion pathway, phosphatidylinositol 3-kinase-Akt signaling (Figure S2) was also highly enriched in SKNs. An important regulator of the cell cycle, this pathway has been implicated in promoting proliferation and inhibiting differentiation in adult hippocampal NPCs (Peltier et al., 2007). Axon guidance was also identified as an enriched pathway between NPCs and SKNs (Figure S3). Ephrins, upregulated in SKNs, have been shown to mediate growth cone survival and collapse, and play a large role in the neural crest migration during gastrulation. EPH-A in particular has also been shown to interact with P75 neurotrophin receptor (P75NTR) in axon guidance and mapping (Lim et al., 2008). In addition, the differentially expressed gene list also contained a number of upregulated genes associated with glutamatergic and GABAergic synapse (Figure S4) pathways, including AMP(A) and GABA(A) postsynaptic receptors, which were both upregulated in SKNs compared with NPCs. Nevertheless, these synaptic pathways in their entirety were not significantly enriched, likely due to the cells' undifferentiated neural precursor phenotype.

SKNs Possess Phenotypic Stability across Cell Lines

As expected, embryonic pluripotency marker NANOG was not expressed. KI67 and SOX2 proliferation markers were present in a majority of SKNs (51% and 72%, respectively), and while OCT4 was highly expressed, staining was perinuclear, consistent with reported expression in dermal cells (Li et al., 2010) (Figures 4A and 4B). SKNs were homogeneous for stem cell-like marker CD133, neural stem/crest cell-like marker NESTIN, and neural crest cell marker P75NTR, a regulatory molecule implicated in both skin stem cell biology (Adly et al., 2009) and neurotrophin signaling (Roux and Barker, 2002) (Figures 4A and 4B). In fact, across these three distinct markers, line-to-line variance was remarkably low: fluorescence-activated cell

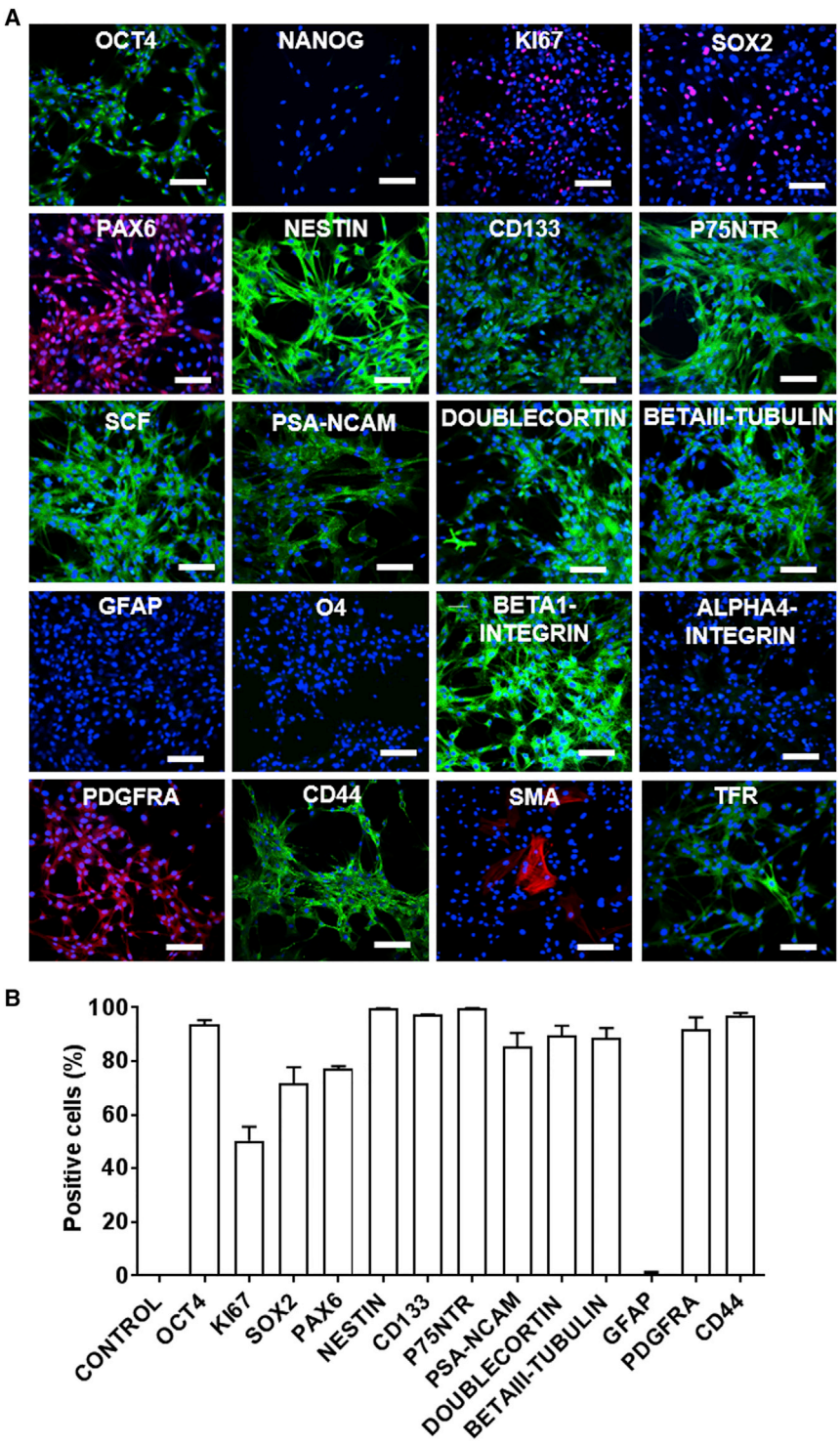

Figure 4. SKNs Homogenously Express Neural Stem Cell-like and Neural Crest Cell Markers

(A) Representative immunocytochemistry images of an array of pluripotency (OCT4 and NANOG), proliferation (KI67 and SOX2), neural stem/precursor cell (PAX6, NESTIN, CD133, P75NTR, SCF, PSA-NCAM, DOUBLECORTIN, BETAIII-TUBULIN), glial cell (GFAP and O4), transmembrane receptors (BETA1-INTEGRIN and ALPHA4-INTEGRIN), and mesenchymal cell markers (PDGFRA, CD44, SMA, and TFR). Nuclei were counterstained with DAPI (blue). Scale bars, 50 μm.

(B) Corresponding flow cytometric quantification showed SKNs were highly homogeneous for neural stem/precursor cell markers (n = 3 independent experiments; mean ± SEM).

sorting of three independent SKN lines (in triplicate) revealed >97% expression for each marker and a between-line coefficient of variance of <1.8%. This excellent level of line-to-line phenotypic replicability is therefore consistent with therapeutic usage.

SKNs also highly expressed an array of neural precursor markers: polysialylated neuronal cell-adhesion molecule (PSA-NCAM), DOUBLECORTIN, and immature neuronal BETAIII-TUBULIN were present in over 85% of cells. Of note, the astrocyte marker glial fibrillary acidic protein

(GFAP) and oligodendrocyte marker O4 were observed in less than 1% of cells (Figure 4A). Expression of BETA1-INTEGRIN, combined with the absence of ALPHA4-INTEGRIN expression, may indicate a propensity of SKNs to preferentially bind laminins. This supports upregulated laminin-associated genes observed within the ECM-receptor-enriched pathway (Figure S5). Mesenchymal markers, platelet-derived growth factor receptor alpha (PDGFRA) and CD44 were found to be expressed in SKNs (Figures 4A and 4B). These proteins were found to be co-expressed with NSC markers CD133 and P75NTR within single cells (Figure S6). Of note, PDGFRA, while classically a mesenchymal marker, is also found in neuroepithelial cells (Andræ et al., 2001) and adult neural precursors. Moreover, adult human PDGFRA-expressing neural precursors of the periventricular region do not co-express GFAP (Chojnacki and Weiss, 2004), and so SKNs may share this non-glial propensity. Expression of mesenchymal myofibroblast marker smooth muscle actin was minimal. Transferrin receptor, traditionally considered a haematopoetic stem cell marker, was also observed in SKNs, although this receptor is also associated with neural cell types throughout the CNS (Erickson et al., 2008).

SKNs Are Neuronally Fate Restricted *In Vitro*

Following passage 3, the proliferative rate of SKNs declines rapidly and their morphology increasingly comes to resemble differentiating neurons. This spontaneous neuronal differentiation was enhanced through the removal of mitogens from the culture medium and supplementation with brain-derived neurotrophic factor (BDNF), known to support neuronal differentiation. Over a 28-day differentiation period, SKNs remained viable, and developed increasingly more complex elongated processes and mature neuronal morphology (Figure 5A), significantly more frequent than in NPCs ($p < 0.0001$; Figure 5B). Post-differentiation SKNs were also a more homogeneous population than NPCs. SKNs expressed neuronal marker genes *TUBB3* and *MAP2* but, unlike differentiated NPCs, glial cell *GFAP* was not expressed (Figure 5C). Mature neuronal gene *ENO2* was expressed in both cultures, while GABAergic gene *GAD67* was only present in differentiated SKNs. Protein expression corroborated these findings (Figure 5D). Mature neuronal proteins NEUN and neurofilament were seen in differentiated SKNs. BETAIII-TUBULIN and MAP2 co-expression can also be seen in morphologically immature (Figure 5D; left) and mature stage differentiated SKNs (Figure 5D; right), while peripheral nervous system (PNS) neuron markers peripherin and P75NTR (when co-expressed with a neuronal cytoskeletal marker, Fernandes et al., 2004) were not present. PNS glial protein MBP (Schwann cells), and CNS glial proteins GFAP (astrocytes) and OLIG2 (oligodendrocytes) were also absent. Positive control stains for these proteins can be seen in Figure S7. Presynaptic vesicular protein BASSOON and punctate accumulation of the FM4-64FX membrane-affinity dye was also detected along the length of the cell processes as well as internalized within the soma, indicative of synaptic vesicle turnover (Figure 5E).

qPCR analysis following differentiation revealed downregulation of proliferative markers *NES* (3-fold; ****$p = 0.0001$) and *P75NTR* (4.9-fold; **$p = 0.001$), complemented by upregulation of the p21 gene *CDKN1A* (4.8-fold; **$p = 0.007$), signifying terminal differentiation (Figure 5F). Notably, significant upregulation of neural specification gene *ASCL1* was observed (27.8-fold; *$p = 0.04$), as well as trends toward increased expression for *POU3F2*, *MYT1L*, and *NEUROD*. SKN differentiation was also accompanied by upregulation of oligodendrocyte repressor gene *DLX2*, and of several neurotransmitter-associated genes including glutamate transporter *SLC17A7*, monoamine transporter *SLC18A2*, GABA receptor *GABBR2* (4.1-fold; *$p = 0.01$), and dopamine transporter *DAT1*. Significant upregulation of the BASSOON gene *BSN* (5-fold; *$p = 0.03$), and a trend toward upregulation of the voltage-gated sodium channel gene *SCN8A*, was also indicative of neuronal maturation (Figure 5F). Overall, these protein and gene expression patterns suggest that canine SKNs are highly neuronally committed.

Differentiated SKNs Possess Basic Neuronal and Synaptic Functionality *In Vitro*

Over the differentiation period, SKNs displayed a steady hyperpolarization of resting membrane potential, with the majority of cells exhibiting resting membrane potentials analogous to mature functional neurons (≥ -55 mV) at 25–28 days *in vitro* (Figure 6A). Functional voltage-gated ion channels were observed under voltage-clamp conditions (Figure 6B), and sub-threshold depolarization and graded regenerative responses were observed via current-clamp recordings as early as 14 days *in vitro* (Figure 6C). However, under these conditions mature action potentials were not recorded, and as such SKNs remained in an electrophysiologically immature neuronal state.

Calcium (Ca^{2+}) influx via voltage-gated channels is known to accompany action potentials. Fura-2-acetoxymethyl ester calcium-affinity dye was therefore used as a higher-throughput method for detection of voltage-gated events. Calcium entry was observed by change in the 340/380 florescence signal ratio over time (Figure 6D) and focal shifts in pseudocolorized image intensity (Figure 6E), when normalized to baseline T0. Differentiated SKNs exposed to a depolarization solution of 129 mM KCl and 2 mM Ca^{2+} show rapid Ca^{2+} internalization (+). Interestingly, depolarization solution containing 100 μM ATP (++) induced an increased influx of Ca^{2+}, with repeated

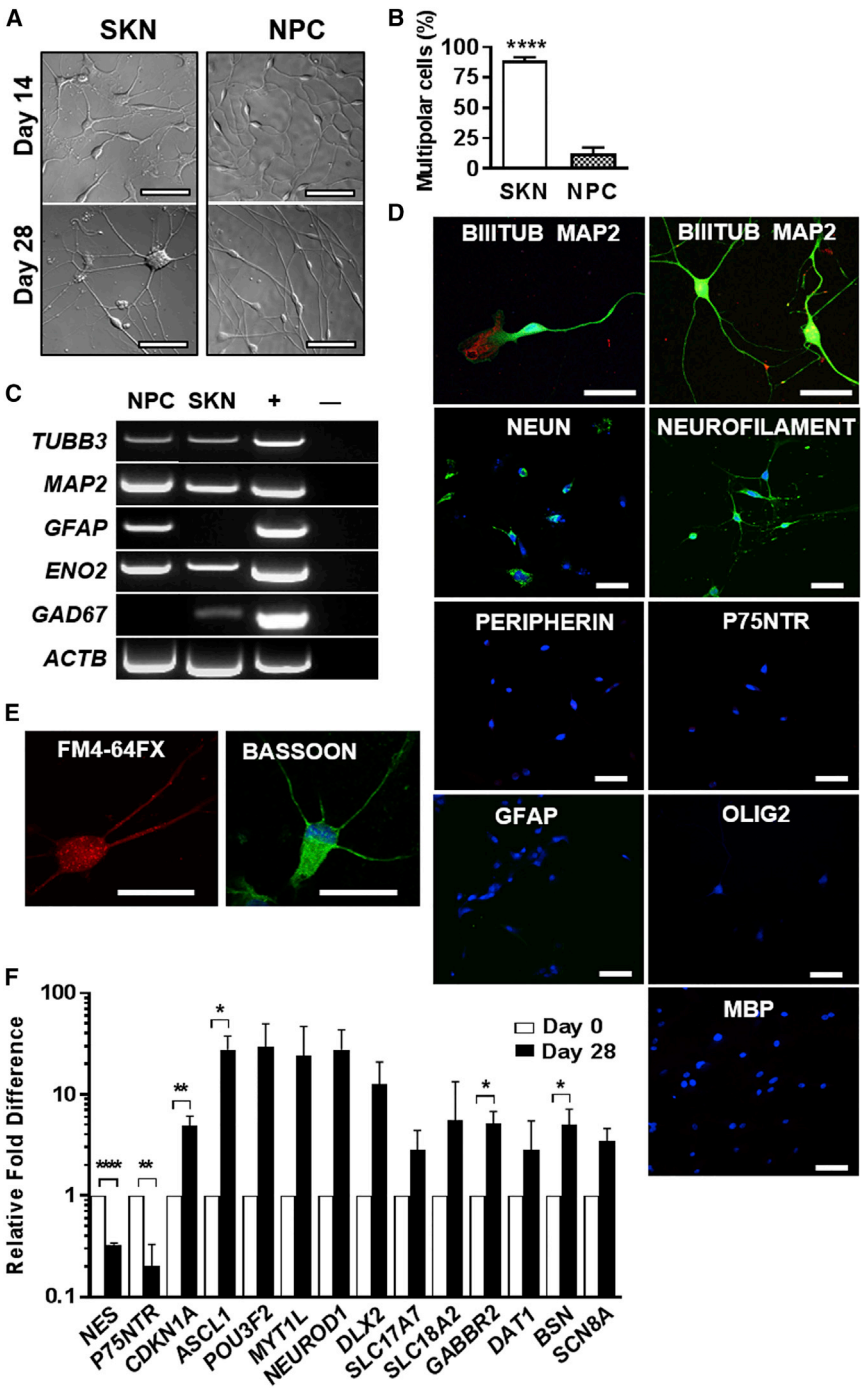

Figure 5. SKNs Are Neuronally Fate Restricted and Endogenously Upregulate Neuronal Specification Genes Following Differentiation

(A) Representative images of SKN and NPC morphology at differentiation days 14 and 28. Scale bars, 50 μm.

(B) Quantitative data of multipolar cell morphology in 28 day differentiated SKNs and NPCs. (****$p < 0.0001$; $n = 3$ independent experiments; mean ± SEM).

(C) Gene expression analysis shows differentiated SKNs and NPCs both express mature neuronal genes. Unlike NPC cultures, SKNs also expressed GABAergic neuronal gene *GAD67*, and did not express glial marker gene *GFAP*. Canine brain isolate was used as a positive control and water a negative control.

(D) Representative immunocytochemistry images of mature neuronal proteins BETAIII-TUBULIN (green) and MAP2 (red), NEUN, and NEUROFILAMENT. PNS neuronal proteins PERIPHERIN and P75NTR (same double stain as NEUROFILAMENT), and both CNS and PNS glial proteins GFAP, OLIG2, and MBP were not expressed in differentiated SKNs. For positive controls stains of these proteins see Figure S7. Scale bars, 50 μm.

(E) Punctate vesicle loading of membrane-affinity dye FM4-64FX within a differentiated SKN cell's neurites and soma, and expression of presynaptic vesicular protein BASSOON. Scale bars, 25 μm.

(F) Differentiated SKNs downregulated neural stem cell genes *NES* (****$p = 0.0001$) and *P75NTR* (**$p = 0.001$), and upregulated cell-cycle exit gene *CDKN1A* (**$p = 0.007$), known neuronal specification genes *ASCL1* (*$p = 0.04$), *POU3F2, MYT1L*, and *NEUROD1,* oligodendrocyte repressor gene *DLX2*, neurotransmitter-associated genes *SLC17A7, SLC18A2, GABBR2* (*$p = 0.01$), and *DAT1*, BASSOON gene *BSN* (*$p = 0.03$), and brain-specific voltage-gated sodium channel gene *SCN8A* ($n = 3$ independent experiments; mean ± SEM).

spikes of calcium entry observed consistent with repeated voltage-gated events.

DISCUSSION

Adult skin is extraordinarily complex, comprised of several interactive stem cell niches that originate from ectodermal, mesenchymal, and neural crest cell lineages. Here, we show that the canine dermis can be used to isolate and propagate precursor cells that display an interesting combination of neural crest, neural stem, and mesenchymal markers. Further, SKN cell lines can be reliably produced from mature dogs, display a high degree of line-to-line stability, are homogeneous across multiple phenotypic markers, and *in vitro* are highly neuronally committed. SKNs are

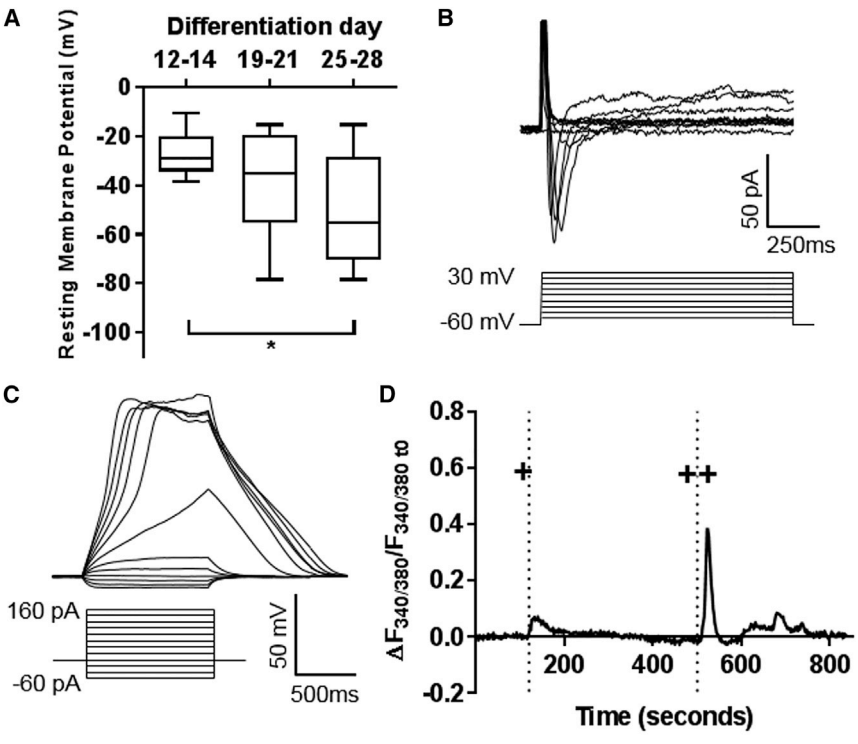

Figure 6. Differentiated SKNs Develop Basic Neuronal and Synaptic Functionality

(A) SKN resting membrane potential hyperpolarized and approached physiological neuronal levels (≥ -55 mV) during 28 days of differentiation (each time point represents readings from >10 individual cells across n = 3 independent experiments). From *post hoc* analysis of multiple comparisons, days 25–28 were significantly different to days 12–14 only ($F_{2,\ 39} = 4.28$, *p = 0.02; mean ± SEM).

(B) Example voltage-clamp recordings illustrating inward and outward voltage-gated ion channel currents in differentiated SKNs.

(C) Current-clamp recordings of regenerative action potentials in a differentiated SKN.

(D) Change in Fura-2AM calcium-affinity dye fluorescence intensity over time, demonstrated functional calcium channel response to (+) a depolarizing solution and potentiation of this response following (++) ATP-based co-activation.

(E) Pseudocolor visualization of (D).

therefore a promising candidate for neural cell therapeutic applications.

Embryologically, brain and skin originate from the same ectodermal lineage. Many adult tissues, including skin, continue to harbor populations of multipotent stem cells. Rather than being necessarily restricted to the tissue-specific lineages of origin, an increasing number of studies suggest that their differentiation potential is diverse and strongly influenced by environmental stimuli. For example, under defined culture conditions, dental pulp stem cells are capable of generating CNS neurons, yet are neural crest-derived and accordingly developmentally restricted to the PNS (Arthur et al., 2008). Similar plasticity is seen in dermal-derived precursor cells. When SKPs (closely related to SKNs) are isolated from neural crest-derived skin tissue they generate not only PNS neural cell types but also CNS neurons (De Kock et al., 2011), and even mesenchymal osteogenic cells (Lavoie et al., 2009). The converse is also possible: the dermal stem cell niche in ventral abdominal skin is non-neural crest in origin yet, despite this, SKPs derived from this niche are capable of generating neural crest-derived cell types (Jinno et al., 2010). SKNs in our study were isolated from ventral skin and therefore are likely to originate from the same non-neural crest-derived multipotent stem cells as ventral SKP cells.

Despite their similar origins, SKNs have several advantages over SKPs from a therapeutic perspective, including reliable homogeneous culture and strong neurogenic bias. Adherent culture is one potential reason for this increased

uniformity, as observed in studies of neurogenic cells (Joannides et al., 2004; Conti et al., 2005; Pollard et al., 2006; Goffredo et al., 2008). In our case, uniformity was seen both within and across lines. We observed less than 2% coefficient of variance for three key phenotypic markers (CD133, NESTIN, and P75NTR) across multiple cell SKN lines and have, to date, produced more than 50 such lines from different dogs with a greater than 85% success rate. Furthermore, for several markers (P75NTR, CD133, and NESTIN), the level of positive expression was >97%, confirming that our protocol produces a reliably homogeneous SKN culture as required for clinical studies.

The pattern of SKN cell marker expression was unique, reflecting both their NPC-like properties (NESTIN and CD133) and dermal origins (PDGFRA and CD44). This pattern has some precedence, with human MSCs shown to spontaneously express neural linage markers SOX2, NESTIN, BETAIII-TUBULIN, and NEUROFILAMENT *in vitro* (Deng et al., 2006; Okolicsanyi et al., 2015). More generally, SKNs also exhibit upregulated and even unique expression of several genes associated with cell proliferation, cell adhesion, and cell migration. SKNs are hence an enriched population of neurogenic cells that may be well suited for survival and migration *in vivo*, a key factor that now requires empirical testing. Importantly, the absence of any genetic manipulation and observation that cell doubling tends to self-limit after four to five passages alongside downregulation of SOX2 further supports the safe use of these cells.

We found that SKNs are fate restricted by virtue of almost exclusive neuronal differentiation. Differentiated cells expressed a range of mature neuronal markers including synaptic and neurotransmitter-associated proteins. While these protein markers can also be found in PNS neurons, the absence of specific peripheral neuronal and glial proteins suggests that SKNs can mature *in vitro* into neurons compatible with the CNS. This neuronal fate bias may be linked to the endogenous upregulation of oligodendrocyte repressor gene, *DLX2* (Petryniak et al., 2007), and spontaneous upregulation of several neural specification genes in response to a differentiation stimuli (high-dose BDNF). Indeed, these specification genes encode for the same four transcription factors (ASCL1, BRN2, MYTL1, and NEUROD) necessary for direct conversion of human somatic cells to iNs (Pang et al., 2011).

Differentiated SKNs also possessed basic neuronal functionality including voltage-gated ion channels and ATP-potentiated calcium transients, as seen in CNS neurons (Lin et al., 2007). However, mature action potentials remained elusive, suggesting that extended differentiation may be necessary for complete functional maturation into definitive neuronal subtypes. Indeed, embryonic stem cell-derived neural precursors have reportedly required up to 7 weeks to develop mature action potentials (Johnson et al., 2007). Nevertheless, global and focal gene expression data suggested that SKNs may possess a GABAergic and glutamatergic neuronal differentiation bias. This is in line with reports that similar adherent expansion of neural stem cells induces a bias toward GABAergic neurons (Goffredo et al., 2008), an intriguing finding that can be followed up in future work. In general, we hope that the strong neurogenic potential of canine SKN cells can be exploited to overcome one of the more pressing deficits in the cell replacement field: poor neuronal yields and an *in vivo* bias toward glial differentiation (Hofstetter et al., 2005; Blurton-Jones et al., 2009).

In summary, SKNs are capable of generating rich and uniform yields of mature neurons comparable with CNS neurons and may therefore have a role in replacement of lost brain cells. Having thoroughly characterized canine SKNs *in vitro*, we are now well placed to determine whether they are affected by disease-related signals and capable of generating structurally and functionally mature neurons *in vivo*.

EXPERIMENTAL PROCEDURES

Cell Culture

Mature dogs up to 6 years of age had abdominal skin tissue ($\approx$6 cm^2) harvested following owner consent. Abdominal skin has been shown to harbor neurogenic stem cells (Toma et al., 2001; Fernandes et al., 2004; Valenzuela et al., 2008; Jinno et al., 2010) and is a practical region for future human clinical study as it is not frequently exposed to potentially mutagenic sunlight (UV radiation), and would represent a less-invasive harvest procedure for aged patients than alternatives such as facial skin (Fernandes et al., 2004). Canine tissue use was approved by the Animal Care and Ethics Committee of the University of New South Wales.

Skin biopsies were divided into 1–2 mm^2 pieces and digested in 0.1% Trypsin (Thermo Fisher Scientific Australia Pty Ltd, Scorseby, VIC, Australia) for 40 min at 37°C, followed by 0.1% DNAse (Roche Applied Science, Castle Hill, NSW, Australia) for 1 min at room temperature. The tissue was then mechanically dissociated and passed through a 40 μm cell strainer (BD Bioscience, Sydney, NSW, Australia), and centrifuged at 180 × *g* for 5 min.

SKNs were then established using our published protocol (Valenzuela et al., 2008). In brief, the dissociated cells were then re-suspended in serum-free complete medium consisting of 3:1 DMEM/Ham's F-12 Nutrient Mixture (DMEM/F12; Thermo Fisher Scientific), 1% Penicillin Streptomycin (Thermo Fisher Scientific), 20 ng/mL EGF (BD Bioscience, Sydney, NSW, Australia), 40 ng/mL bFGF (Thermo Fisher Scientific), and 2% B-27 supplement (Thermo Fisher Scientific). The cells were then seeded at a density of 100,000 cells/cm^2. When resulting neurospheres reached 50–100 μm in diameter, they were dissociated using TrypLE Select (Thermo Fisher Scientific) for 5 min at 37°C. Cells were then re-suspended in complete medium and grown as an adherent monolayer

by seeding at 10,000 cells/cm^2 on 0.1% gelatin-coated flasks, and passaged when 80% confluent.

For FBT culture, the dissociated cells were re-suspended in 3:1 DMEM/F12 medium containing 10% fetal bovine serum (Thermo Fisher Scientific), 1% GlutaMAX (Thermo Fisher Scientific), and 1% penicillin streptomycin. Hereafter referred to as FDMEM, and seeded at a density of 100,000 cells/cm^2.

NPCs were derived from subventricular zone brain isolates, following previously published protocols (Duncan et al., 2016).

Transcriptomic Analysis

RNA from three individual donor lines each of SKNs, NPCs, and FBTs were subjected to genome-wide transcriptomic analysis using an Affymetrix Canine Genechip Gene 1.0 ST array (Affymetrix, Santa Clara, CA, USA). The complete microarray data are available online at https://www.ncbi.nlm.nih.gov/geo/ (accession number GEO: GSE74714).

Immunocytochemistry and Flow Cytometry

Cells fixed with 4% paraformaldehyde were permeabilized in 0.5% Triton X-100 for 30 min, then blocked using 10% normal donkey serum (Sigma-Aldrich, Castle Hill, NSW, Australia) for 1 hr prior to overnight incubation in diluted primary antibodies. Alexo Fluor 488 or 594 secondary antibody (Thermo Fisher Scientific) incubation, and DAPI counterstaining was then carried out prior to imaging on a Leica DMI3000B Microscope, or quantification using a MACSQuant Analyzer flow cytometer (Miltenyi Biotec Pty Ltd, Sydney, NSW, Australia).

Gene Expression

RNA was extracted using an illustra RNAspin Mini Isolation Kit (GE Healthcare, Little Chalfont, Buckinghamshire, UK) according to the manufacturer's instructions. cDNA was synthesized using Superscript III RT First Strand Synthesis System (Thermo Fisher Scientific). PCR amplification was then performed using Platinum *Taq* DNA Polymerase (Thermo Fisher Scientific). qRT-PCR was carried out using the CFX96 Real-Time PCR/C1000 thermal cycler (Bio-Rad Laboratories, Hercules, CA, USA) using SsoFast EvaGreen Supermix (Bio-Rad Laboratories). Relative gene expression was calculated using endogenous *GAPDH* housekeeping gene.

Electrophysiology

Whole-cell patch-clamp recordings were performed on differentiated SKN cells at room temperature (22.5°C ± 0.3°C). All membrane potentials were corrected for the liquid junction potential of 15.4 mV. Recordings were performed using an Axopatch-1D amplifier and digitized using pClamp 10.4 software and a Digidata 1440 interface (Molecular Devices, Sunnyvale, CA, USA) at 10 kHz, and filtered with an 8 pole Bessel filter at 2 kHz.

Calcium Imaging

Fura2-AM dye (Thermo Fisher Scientific) was used as a ratiometric calcium indicator. Fluorescence intensity was recorded while perfused in a 5 mM KCl, 0 mM Ca^{2+} baseline solution, followed by 129 mM KCl, 2 mM Ca^{2+}, then 129 mM KCl, 2 mM Ca^{2+}, and 100 μM ATP solutions.

Statistical Analysis

Repeat experiments were conducted on biologically independent cell lines. Statistical analysis was performed using GraphPad Prism (GraphPad Software, La Jolla, CA, USA), analyzed by Student's t test or ANOVA for multiple comparisons and considered significant at $p < 0.05$.

For further details of experimental procedures see Supplemental Experimental Procedures.

SUPPLEMENTAL INFORMATION

Supplemental Information includes Supplemental Experimental Procedures, seven figures, and three tables and can be found with this article online at http://dx.doi.org/10.1016/j.stemcr.2017.07.008.

AUTHOR CONTRIBUTIONS

T.D. collected data, analyzed and interpreted results, and prepared the manuscript. A.L. and R.C.Y.L. designed the experiments, collected data, analyzed and interpreted results, and prepared the manuscript. K.S. and P.S. designed the experiments and analyzed and interpreted results. T.L., V.S., and M.V. designed the experiments, provided research material/equipment, and analyzed and interpreted results.

ACKNOWLEDGMENTS

This work was supported by the Rebecca L. Cooper Medical Research Foundation, the ANZ Mason Foundation, the National Health and Medical Research Council (NHMRC) of Australia Program Grant (no. 568969), and philanthropic gifts from Ron Sinclair and Alzheimer's Australia. We appreciate the expert contributions of Dr Sandra Fok, Professor Mirjana Maletic-Savatic, and Professor Perry Bartlett.

Received: December 15, 2016
Revised: July 7, 2017
Accepted: July 10, 2017
Published: August 8, 2017

REFERENCES

Adly, M.A., Assaf, H.A., and Hussein, M.R. (2009). Expression pattern of p75 neurotrophin receptor protein in human scalp skin and hair follicles: hair cycle-dependent expression. J. Am. Acad. Dermatol. *60*, 99–109.

Andræ, J., Hansson, I., Afink, G.B., and Nistér, M. (2001). Platelet-derived growth factor receptor-α in ventricular zone cells and in developing neurons. Mol. Cell. Neurosci. *17*, 1001–1013.

Arthur, A., Rychkov, G., Shi, S., Koblar, S.A., and Gronthos, S. (2008). Adult human dental pulp stem cells differentiate toward functionally active neurons under appropriate environmental cues. Stem Cells *26*, 1787–1795.

Babu, H., Cheung, G., Kettenmann, H., Palmer, T.D., and Kempermann, G. (2007). Enriched monolayer precursor cell cultures from micro-dissected adult mouse dentate gyrus yield functional granule cell-like neurons. PLoS One *2*, e388.

Bez, A., Corsini, E., Curti, D., Biggiogera, M., Colombo, A., and Et, A. (2003). Neurosphere and neurosphere-forming cells: morphological and ultrastructural characterization. Brain Res. *993*, 18–29.

Biernaskie, J.A., McKenzie, I.A., Toma, J.G., and Miller, F.D. (2006). Isolation of skin-derived precursors (SKPs) and differentiation and enrichment of their Schwann cell progeny. Nat. Protoc. *1*, 2803–2812.

Blurton-Jones, M., Kitazawa, M., Martinez-Coria, H., Castello, N.A., Muller, F.J., Loring, J.F., Yamasaki, T.R., Poon, W.W., Green, K.N., and LaFerla, F.M. (2009). Neural stem cells improve cognition via BDNF in a transgenic model of Alzheimer disease. Proc. Natl. Acad. Sci. USA *106*, 13594–13599.

Breitner, J.C. (2015). Comment: yet another "disconnect" between amyloid and Alzheimer disease? Neurology *85*, 698.

Chojnacki, A., and Weiss, S. (2004). Isolation of a novel platelet-derived growth factor-responsive precursor from the embryonic ventral forebrain. J. Neurosci. *24*, 10888–10899.

Conti, L., Pollard, S., Gorba, T., Reitano, E., Toselli, M., Biella, G., and Et, A. (2005). Niche-independent symmetrical self-renewal of a mammalian tissue stem cell. PLoS Biol. *3* (9), e283.

Cummings, B.J., Head, E., Ruehl, W., Milgram, N.W., and Cotman, C.W. (1996). The canine as an animal model of human aging and dementia. Neurobiol. Aging *17*, 259–268.

Cummings, J.L., Morstorf, T., and Zhong, K. (2014). Alzheimer's disease drug-development pipeline: few candidates, frequent failures. Alzheimers Res. Ther. *6*, 37–44.

D'Ercole, J.A., Ye, P., and O'Kusky, J.R. (2002). Mutant mouse models of insulin-like growth factor actions in the central nervous system. Neuropeptides *36*, 209–220.

Daley, G.Q. (2012). The promise and perils of stem cell therapeutics. Cell Stem Cell *10*, 740–749.

De Kock, J., Snykers, S., Ramboer, E., Demeester, S., Heymans, A., Branson, S., Vanhaecke, T., and Rogiers, V. (2011). Evaluation of the multipotent character of human foreskin-derived precursor cells. Toxicol. In Vitro *25*, 1191–1202.

Deng, J., Petersen, B.E., Steindler, D.A., Jorgensen, M.L., and Laywell, E.D. (2006). Mesenchymal stem cells spontaneously express neural proteins in culture and are neurogenic after transplantation. Stem Cells *24*, 1054–1064.

Duncan, T., Lowe, A., Dalton, M., and Valenzuela, M. (2016). Isolation and expansion of adult canine hippocampal neural precursors. J. Vis. Exp. http://dx.doi.org/10.3791/54953.

Duncan, T., and Valenzuela, M. (2017). Alzheimer's disease, dementia, and stem cell therapy. Stem Cell Res. Ther. *8*, 111.

Erickson, R.I., Paucar, A.A., Jackson, R.L., Visnyei, K., and Kornblum, H. (2008). Roles of insulin and transferrin in neural progenitor survival and proliferation. J. Neurosci. Res. *86*, 1884–1894.

Esmailpour, T., and Huang, T. (2012). TBX3 promotes human embryonic stem cell proliferation and neuroepithelial differentiation in a differentiation stage-dependent manner. Stem Cells *30*, 2152–2163.

Fernandes, K., McKenzie, I., Mill, P., and Et, A. (2004). A dermal niche for multipotent adult skin-derived precursor cells. Nat. Cell Biol. *6*, 1082–1093.

Goffredo, D., Conti, L., Di Febo, F., Biella, G., Tosoni, A., Vago, G., Biunno, I., Moiana, A., Bolognini, D., and Toselli, M. (2008). Setting the conditions for efficient, robust and reproducible generation of functionally active neurons from adult subventricular zone-derived neural stem cells. Cell Death Differ. *15*, 1847–1856.

Greenwood, S.K., Hill, R.B., Sun, J.T., Armstrong, M.J., Johnson, T.E., Gara, J.P., and Galloway, S.M. (2004). Population doubling: a simple and more accurate estimation of cell growth suppression in the in vitro assay for chromosomal aberrations that reduces irrelevant positive results. Environ. Mol. Mutagen. *43*, 36–44.

Hofstetter, C.P., Holmstrom, N.A., Lilja, J.A., Schweinhardt, P., Hao, J., Spenger, C., Wiesenfeld-Hallin, Z., Kurpad, S.N., Frisen, J., and Olson, L. (2005). Allodynia limits the usefulness of intraspinal neural stem cell grafts; directed differentiation improves outcome. Nat. Neurosci. *8*, 346–353.

Hunt, D.P., Morris, P.N., Sterling, J., Anderson, J.A., Joannides, A., Jahoda, C., Compston, A., and Chandran, S. (2008). A highly enriched niche of precursor cells with neuronal and glial potential within the hair follicle dermal papilla of adult skin. Stem Cells *26*, 163–172.

Jinno, H., Morozova, O., Jones, K.L., Biernaskie, J.A., Paris, M., Hosokawa, R., Rudnicki, M.A., Chai, Y., Rossi, F., Marra, M.A., et al. (2010). Convergent genesis of an adult neural crest-like dermal stem cell from distinct developmental origins. Stem Cells *28*, 2027–2040.

Joannides, A., Gaughwin, P., Schwiening, C., Majed, H., Sterling, J., Compston, A., and Chandran, S. (2004). Efficient generation of neural precursors from adult human skin: astrocytes promote neurogenesis from skin-derived stem cells. Lancet *364*, 172–178.

Johnson, M.A., Weick, J.P., Pearce, R.A., and Zhang, S.-C. (2007). Functional neural development from human embryonic stem cells: accelerated synaptic activity via astrocyte coculture. J. Neurosci. *27*, 3069–3077.

Kanehisa, M., Goto, S., Kawashima, S., Okuno, Y., and Hattori, M. (2004). The KEGG resource for deciphering the genome. Nucleic Acids Res. *32*, 277–280.

Lavoie, J.F., Biernaskie, J.A., Chen, Y., Bagli, D., Alman, B., Kaplan, D.R., and Miller, F.D. (2009). Skin-derived precursors differentiate into skeletogenic cell types and contribute to bone repair. Stem Cells Dev. *18*, 893–906.

Lefebvre, J.L., Kostadinov, D., Chen, W.V., Maniatis, T., and Sanes, J.R. (2012). Protocadherins mediate dendritic self-avoidance in the mammalian nervous system. Nature *488*, 517–521.

Li, L., Fukunaga-Kalabis, M., Yu, H., Xu, X.W., Kong, J., Lee, J.T., and Herlyn, M. (2010). Human dermal stem cells differentiate into functional epidermal melanocytes. J. Cell Sci. *123*, 853–860.

Liao, J., Wu, Z., Wang, Y., Cheng, L., Cui, C., Gao, Y., Chen, T., Rao, L., Chen, S., Jia, N., et al. (2008). Enhanced efficiency of generating induced pluripotent stem (iPS) cells from human somatic cells by a combination of six transcription factors. Cell Res. *18*, 600–603.

Lim, Y.-S., McLaughlin, T., Sung, T.-C., Santiago, A., Lee, K.-F., and O'Leary, D.D. (2008). p75 NTR mediates ephrin-A reverse signaling required for axon repulsion and mapping. Neuron *59*, 746–758.

Lin, J.H.C., Takano, T., Arcuino, G., Wang, X.H., Hu, F.R., Darzynkiewicz, Z., Nunes, M., Goldman, S.A., and Nedergaard, M. (2007).

Purinergic signaling regulates neural progenitor cell expansion and neurogenesis. Dev. Biol. *302*, 356–366.

Lindvall, O., Barker, R.A., Brustle, O., Isacson, O., and Svendsen, C.N. (2012). Clinical translation of stem cells in neurodegenerative disorders. Cell Stem Cell *10*, 151–155.

Michaelson, M.D., Mehler, M.F., Xu, H., Gross, R.E., and Kessler, J.A. (1996). Interleukin-7 is trophic for embryonic neurons and is expressed in developing brain. Dev. Biol. *179*, 251–263.

Okolicsanyi, R.K., Camilleri, E.T., Oikari, L.E., Yu, C., Cool, S.M., van Wijnen, A.J., Griffiths, L.R., and Haupt, L.M. (2015). Human mesenchymal stem cells retain multilineage differentiation capacity including neural marker expression after extended in vitro expansion. PLoS One *10*, e0137255.

Pang, Z.P., Yang, N., Vierbuchen, T., Ostermeier, A., Fuentes, D.R., Yang, T.Q., Citri, A., Sebastiano, V., Marro, S., Sudhof, T.C., et al. (2011). Induction of human neuronal cells by defined transcription factors. Nature *476*, 220–223.

Peltier, J., O'Neill, A., and Schaffer, D.V. (2007). PI3K/Akt and CREB regulate adult neural hippocampal progenitor proliferation and differentiation. Dev. Neurobiol. *67*, 1348–1361.

Petryniak, M.A., Potter, G.B., Rowitch, D.H., and Rubenstein, J.L. (2007). Dlx1 and Dlx2 control neuronal versus oligodendroglial cell fate acquisition in the developing forebrain. Neuron *55*, 417–433.

Pfisterer, U., Wood, J., Nihlberg, K., Hallgren, O., Bjermer, L., Westergren-Thorsson, G., Lindvall, O., and Parmar, M. (2011). Efficient induction of functional neurons from adult human fibroblasts. Cell Cycle *10*, 3311–3316.

Pollard, S., Conti, L., Sun, Y., Goffredo, D., and Smith, A. (2006). Adherent neural stem (NS) cells from foetal and adult forebrain. Cereb. Cortex *16*, i112–i120.

Reynolds, B., and Rietze, R. (2005). Neural stem cells and neurospheres – re-evaluating the relationship. Nat. Methods *2*, 333–336.

Ring, K.L., Tong, L.M., Balestra, M.E., Javier, R., Andrews-Zwilling, Y., Li, G., Walker, D., Zhang, W.R., Kreitzer, A.C., and Huang, Y. (2012). Direct reprogramming of mouse and human fibroblasts into multipotent neural stem cells with a single factor. Cell Stem Cell *11*, 100–109.

Rosenstein, J.M., Krum, J.M., and Ruhrberg, C. (2010). VEGF in the nervous system. Organogenesis *6*, 107–114.

Roux, P.P., and Barker, P.A. (2002). Neurotrophin signaling through the p75 neurotrophin receptor. Prog. Neurobiol. *67*, 203–233.

Salvin, H.E., McGreevy, P.D., Sachdev, P.S., and Valenzuela, M.J. (2010). Under diagnosis of canine cognitive dysfunction: a cross-sectional survey of older companion dogs. Vet. J. *184*, 277–281.

Salvin, H.E., McGreevy, P.D., Sachdev, P.S., and Valenzuela, M.J. (2011). The canine cognitive dysfunction rating scale (CCDR): a data-driven and ecologically relevant assessment tool. Vet. J. *188*, 331–336.

Sano, K., Tanihara, H., Heimark, R.L., Obata, S., Davidson, M., St John, T., Taketani, S., and Suzuki, S. (1993). Protocadherins: a large family of cadherin-related molecules in central nervous system. EMBO J. *12*, 2249–2256.

Schalm, S.S., Ballif, B.A., Buchanan, S.M., Phillips, G.R., and Maniatis, T. (2010). Phosphorylation of protocadherin proteins by the receptor tyrosine kinase Ret. Proc. Natl. Acad. Sci. USA *107*, 13894–13899.

Scheff, S.W., and Price, D.A. (2006). Alzheimer's disease-related alterations in synaptic density: neocortex and hippocampus. J. Alzheimers Dis. *9*, 101–115.

Takahashi, K., Tanabe, K., Ohnuki, M., Narita, M., Ichisaka, T., Tomoda, K., and Yamanaka, S. (2007). Induction of pluripotent stem cells from adult human fibroblasts by defined factors. Cell *131*, 861–872.

Takahashi, K., and Yamanaka, S. (2006). Induction of pluripotent stem cells from mouse embryonic and adult fibroblast cultures by defined factors. Cell *126*, 663–676.

Terry, R.D., Masliah, E., Salmon, D.P., Butters, N., DeTeresa, R., Hill, R., Hansen, L.A., and Katzman, R. (1991). Physical basis of cognitive alterations in Alzheimer's disease: synapse loss is the major correlate of cognitive impairment. Ann. Neurol. *30*, 572–580.

Toma, J.G., Akhavan, M., Fernandes, K.J., Barnabe-Heider, F., Sadikot, A., Kaplan, D.R., and Miller, F.D. (2001). Isolation of multipotent adult stem cells from the dermis of mammalian skin. Nat. Cell Biol. *3*, 778–784.

Toma, J., McKenzie, I., Bagli, D., and Miller, F. (2005). Isolation and characterization of multipotent skin-derived precursors from human skin. Stem Cells *23*, 727–737.

Truong, A., Si, E., Duncan, T., and Valenzuela, M. (2016). Modeling neurodegenerative disorders in adult somatic cells: a critical review. Front. Biol. *11*, 232–245.

Valenzuela, M.J., Dean, S.K., Sachdev, P., Tuch, B.E., and Sidhu, K.S. (2008). Neural precursors from canine skin: a new direction for testing autologous cell replacement in the brain. Stem Cells Dev. *17*, 1–8.

Wernig, M., Zhao, J.P., Pruszak, J., Hedlund, E., Fu, D., Soldner, F., Broccoli, V., Constantine-Paton, M., Isacson, O., and Jaenisch, R. (2008). Neurons derived from reprogrammed fibroblasts functionally integrate into the fetal brain and improve symptoms of rats with Parkinson's disease. Proc. Natl. Acad. Sci. USA *105*, 5856–5861.

Xia, N., Thodeti, C.K., Hunt, T.P., Xu, Q., Ho, M., Whitesides, G.M., Westervelt, R., and Ingber, D.E. (2008). Directional control of cell motility through focal adhesion positioning and spatial control of Rac activation. FASEB J. *22*, 1649–1659.